medium pressure Hg lamp for 6 hr furnished a 5.5 : 4.5 mixture of **2** and **3** in more than 99% yield, together with negligible other products.

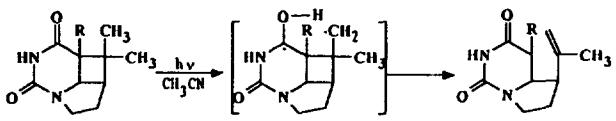

**2** **5** **3**

Irradiation of **1** with a 12W low pressure Hg lamp gave the same result. The detailed consequence of the resulting photocycloaddition will be published in a forthcoming paper. Unambiguous assignment of the structure of **3a** was performed by single-crystal X-ray diffraction techniques.[5]

The structure was proved to be fused by a $N^1$-C6 bond of 5- and 6- membered ring and to have a butterfly conformation with an almost planar pyrimidone part (Figure 1). Two molecules are held together by an inversion center through two hydrogen bonding interactions between N and O atoms of pyrimidine moiety (Figure 2).

**Acknowledgment.** The structural study of this work was supported by the Korea Science and Engineering Foundation (KOSEF).

## References

1. (a) Schuster, D. I.; Len, G.; Kaprinidins, N. A. *Chem. Rev.* **1993**, *93*, 3. (b) Becker, D.; Haddad, N. *Org. Photochem.* **1989**, *10*, 1. (c) Crimmins, M. T. *Chem. Rev.* **1988**, *88*, 1453. (d) Carless, H. A. *Photochemistry in Organic Synthesis*; Coyle, J. D.; Royal Soc. Chem: London. **1986**; p 95-117. (e) Weeden, A. C. *Synthetic Org. Chemistry*; Horspool, W. M., Ed., Plenum Press; New York, **1984**, p 61-144. (f) Oppolzer, W. Acc. *Chem. Res.* **1982**, *15*, 135. (g) Boldwin, S. W. *Org. Photochem.* **1981**, *5*, 23.
2. (a) Ikeda, M.; Uchiro, T.; Takahashi, M.; Ishibashi, H.; Tamura, Y.; Kido, M. *Chem. Pharm. Bull.* **1985**, *33*, 3279. (b) Ikeda, M. ; Takahashi, H. Uchiro, T.; Ohro, K.; Tamura, Y.; Kido, M. *J. Org. Chem.* **1982**, *47*, 3597. (c) Coates, R. M.; Senter, P. D.; Baker, W. R. *J. Org. Chem.* **1983**, *47*, 3597. (d) Begley, M. J.; Mellor, M.; Pattender, G. *J. Chem. Soc., Chem. Commun.* **1979**, 235. (e) Tamura, Y.; Ishibashi, H.; Hirai, M.; Kita, Y.; Iketa, M. *J. Org. Chem.* **1975**, *40*, 2702. (f) Tamura, Y.; Kita, Y. Isibashi, H.; Keta, M. *J. Chem. Soc., Chem. Commun.* **1971**, 1167.
3. (a) Ahn, C. I.; Choi, H.; Hahn, B. S. *Heterocycles.* **1990**, *31*, 1737. (b) **1a**: yield 42%; mp 118-119 ℃ ; $^1$H NMR (80 MHz, $CDCl_3$) δ 1.56 (s, 3H), 1.72 (s, 3H), 2.38 (q, $J$=6.8 Hz, 2H), 3.70 (t, $J$=7.2 Hz, 2H), 4.97-5.18 (m, 1H), 5.64 (d, $J$=8.8 Hz, 1H), 8.86 (s, 1H); IR (KBr), 1690, 1638 $cm^{-1}$ ($\nu_{C=O}$); EIMS m/z 194 ($M^+$). **1b**: yield 46%; mp 159-160 ℃ ; $^1$H NMR (80 MHz, $CDCl_3$) δ 1.59 (s, 3H), 1.71 (s, 3H), 1.88 (s, 3H), 2.35 (q, $J$=12.4 Hz, 2H), 3.67 (t, $J$=6.8 Hz, 2H), 4.93-5.17 (m, 1H), 6.83 (s, 1H), 8.70 (s, 1H); IR (KBr), 1685, 1643 $cm^{-1}$ ($\nu_{C=O}$); EIMS m/z 208 ($M^+$).
4. **2a**: yield 37%; mp 168-170 ℃ ; $^1$H NMR (200 MHz, $CDCl_3$) δ 0.90 (s, 3H), 1.28 (s, 3H), 1.84-1.94 (m, 2H), 2.63 (td, $J$=6.2, 5.7 Hz, 1H), 2.83 (d, $J$=5.8 Hz, 1H), 3.13 (ddd, $J$=12.2, 8.7, 8.7 Hz, 1H), 3.91 (dd, $J$=5.7, 5.6 Hz, 1H), 4.05-4.17 (m, 2H), 7.18 (s, 1H); IR (KBr), 1713, 1683 $cm^{-1}$ ($\nu_{C=O}$); EIMS m/z 194 ($M^+$). **2b**: yield 33%; mp 204-206 ℃ ; $^1$H NMR (200 MHz, $CDCl_3$) δ 0.90 (s, 3H), 1.05 (s, 3H), 1.34 (s, 3H), 1.82-1.93 (m, 2H), 2.61 (td, $J$=6.1, 5.6 Hz, 1H), 3.16 (ddd, $J$=12.2, 8.7, 8.7 Hz, 1H), 3.55 (d, $J$=6.2 Hz, 1H), 4.06-4.19 (m, 1H), 7.20 (s, 1H); IR (KBr), 1703 $cm^{-1}$ ($\nu_{C=O}$); EIMS m/z 208 ($M^+$). **3a**: yield 45%; mp 148-150 ℃ ; $^1$H NMR (200 MHz, $CDCl_3$) δ 1.67 (d, $J$=0.7 Hz, 3H), 1.90-2.11 (m, 2H), 2.22-2.47 (m, 2H), 2.85-2.94 (m, 1H), 3.41-3.53 (m, 1H), 3.61-3.75 (m, 1H), 3.85-3.98 (m, 1H), 4.72 (s, 1H), 4.92 (dd, $J$=1.31, 1.1 Hz, 1H), 7.78 (s, 1H); IR (KBr), 1713, 1693 $cm^{-1}$ ($\nu_{C=O}$); EIMS m/z 194 ($M^+$). **3b**: yield 41%; mp 220-222 ℃ ; $^1$H NMR (200 MHz, $CDCl_3$) δ 1.10 (d, $J$=6.7 Hz, 3H), 1.67 (s, 3H), 1.90-2.18 (m, 2H), 2.32-2.42 (m, 1H), 2.89 (dd, $J$=6.3, 6.2 Hz, 1H), 3.45 (dd, $J$=12.7, 5.8 Hz, 1H), 3.54-3.62 (m, 2H), 4.70 (s, 1H), 4.86 (d, $J$=1.3 Hz, 1H), 7.17 (s, 1H); IR (KBr), 1721, 1691 $cm^{-1}$ ($\nu_{C=O}$); EIMS m/z 208 ($M^+$).
5. Data for crystallographic studies were measured on a MAC sciences MXC[3] four-circle diffractometer. The unit cell and other related parameters of compound (3a) are as follows; F.W=194.23; Coloress plate; Crystal dimension=1.0×1.0×0.2 $mm^3$; Space group $P2_1/n$ (No. 14); $a$=14.456 (5) Å, $b$=7.999 (3) Å, $c$=8.858(3) Å, β=100.58 (3)°, V=1006.9 (5) $Å^3$; Z=4; $D_{calc}$=1.28 $mg/m^3$; Radiation=MoKα, λ=0.71069 Å; μ=0.091 $mm^{-1}$; F(000)=416; Temperature=293 K; Final R=0.0367; Number of unique reflections=1582.

## Prediction of Asymmetric Resonances in the Predissociation of the $A^2\Sigma^+$ State of OH

Sungyul Lee

*Department of Chemistry, Kyunghee University, Kyungki-do 449-701, Korea*

*Received January 26, 1995*

Photodissociation to open-shell atomic fragments has yielded valuable informations on the nonadiabatic interactions among electronically excited states.[1,2] When the fragments have nonvanishing angular momenta, there may be more than one electronic state correlating with an atomic term limit. Nonadiabatic interactions among these states can affect the dissociation processes since these interactions can be equal to or larger than the separations between the electronic states at intermediate and asymptotic internuclear distances. Freed and coworkers[2~5] have shown for direct dissociation processes that the nonadiabatic couplings could affect the outcomes of the dissociation processes, such as the population ratios of the atomic fine structure components and the anisotropy parameters.

When there is an explicit curve crossing between states correlating with different atomic term limits, as in predissociating systems, *two* different kinds of nonadiabatic interactions must be considered. The influence of the interactions

in the Franck-Condon region between crossing states, correlating to *different* atomic term limits, are significant near the crossing point. It is well known that these interactions between binding and dissociative states basically determine the widths and positions of the resonances (or quasibound states). They may also affect the shape of the resonances when the dissociative states are optically coupled with the initial state.[6] Depending on the interactions, resonances can exhibit a variety of non-Lorentzian profiles. These so-called Fano profiles[6] have been observed in the predissociation of $H_2$,[7] $Cs_2$[8] and FNO.[9] On the other hand, nonadiabatic interactions among states approaching the *same* atomic term limit become important at large interunclear distances. Lee *et al.*[10] have shown in a model calculation for OH predissociation processes that the nonadiabatic interactions between states correlating with $O(^3P)$ term exhibit profound influence on the population ratios of the oxygen fine structure states $O(^3P_j, j=0, 1, 2)$. These two types of nonadiabatic interactions are expected to affect the outcomes of the dissociation dynamics in a very complicated way.

The theory of diatomic photodissociation to atomic fine structure states has been described by Singer *et al.*[1] for direct dissociation processes. Recently, we have developed[11] an *exact* theory to treat the predissociation processes, where at least two atomic term limits are involved. Details of the theory will be described elsewhere,[11] and we only give a brief summary in this Communication. The basic ingredient of the theory is the transformation matrices that connect each of the atomic term limits to adiabatic Born-Oppenheimer (ABO) states that correlate with it. For OH predissociation *two* transformation matrices are needed, since two atomic term limits (that is, $O(^3P)$ and $O(^1D)$) are involved in the dissociation process. Two kinds of basis functions are used in the calculations to evaluate the total Hamiltonian. Hund's case (a) basis function of parity $p$, $|JMC\Lambda S\Sigma p\rangle$ is employed to evaluate the electronic Hamiltonian, which is diagonal in this basis. The asymptotic basis functions $|JMjlC_O j_O j_H\rangle$ are used to evaluate the spin-orbit Hamiltonian and the rotational part $l(l+1)/2\mu r^2$, since they are diagonal in these basis functions. Here $j_O$ ($j_H$) are the total electronic angular momentum of the oxygen (hydrogen) fragment and $l$ is the orbital angular momentum, $j=j_O+j_H$, and $C_O$ denotes extra quantum numbers needed to describe the electronic states of the oxygen atom besides $j_O$ (that is, spin and electronic orbital angular momentum quantum numbers). The two basis functions are related to each other by $r$-independent transformation matrices $\langle jlC_O j_O j_H|C\Lambda S\Sigma p\rangle_J$. Spin-orbit and Coriolis couplings among ABO states correlating to the same atomic term limit are assumed to have their asymptotic values at all internuclear distances. Since the influences of these couplings are only significant in asymptotic region, this assumption is expected to hold very well. Close-coupled equations are solved for the multichannel continuum wavefunction of energy $E$. The continuum wavefunction is propagated in the ABO basis $|JMC\Lambda S\Sigma p\rangle$ using the Renormalized Numerov method.[12] The transition amplitudes in ABO basis are transformed into the asymptotic basis $|JMjlC_O j_O j_H\rangle$ by the two frame transformation matrices at the end of the propagation and appropriate boundary conditions are imposed. The transition amplitudes for dissociation to a specific fine structure component of the oxygen atom is calculated by employing the

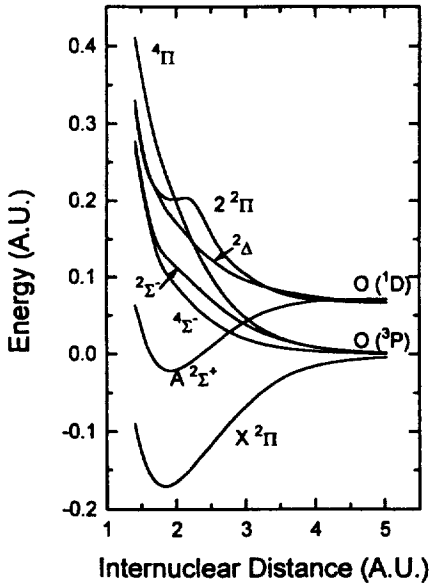


**Figure 1.** Potential curves of OH.

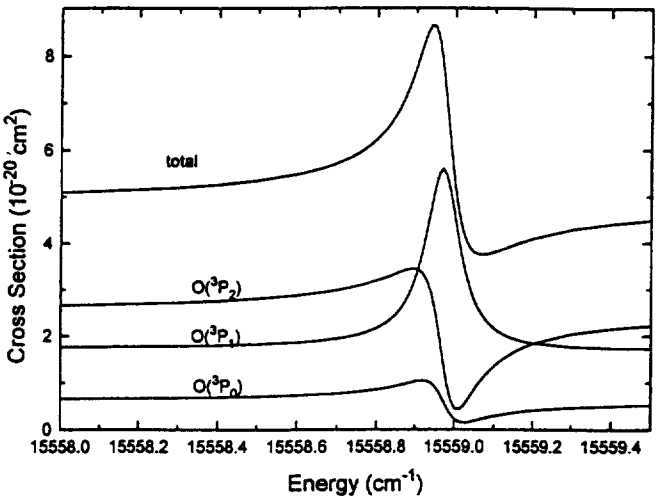


**Figure 2.** Resonance corresponding to the $F_2$ level ($J_f=5/2$) with $N=2$ and $v=9$ of the $A^2\Sigma^+$ state.

Golden Rule. Cooley's method[13] is used to evaluate the initial bound state vibrational wave function of the $X^2\Pi$ state.

Figure 1 depicts the potential curves of the OH molecule that are involved in the OH predissociation processes. The ground $X^2\Pi$ state and repulsive states $^4\Sigma^-$, $^2\Sigma^-$ and $^4\Pi$ correlate with triplet oxygen $O(^3P)$, while the $A^2\Sigma^+$, $^2\Delta$ and $2^2\Pi$ states correlate with the singlet oxygen $O(^1D)$. Predissociation of the rovibrational levels of the $A^2\Sigma^+$ state results from the spin-orbit coulplings between the $A^2\Sigma^+$ and the three repulsive states $^4\Sigma^-$, $^2\Sigma^-$ and $^4\Pi$. Figure 1 shows that the Franck-Condon overlap of the $^2\Sigma^-$ state with the $X^2\Pi$ state is very small for energies near the lower rovibrational levels of the $A^2\Sigma^+$ state. Our calculations predict that the resonances in this lower energy regime are Lorentzian, and the calculated nonradiative lifetimes of these resonances agree well with experimental results.[11(c)] For higher rovibrational levels, however, the Franck-Condon overlap increases, and so the dissociative $^2\Sigma^-$ state is expected to carry appre-

ciable oscillator strength from the ground state. Our calculations indicate that for states with $v \geq 7$, the resonances will show asymmetric features due to the quantum interference between the binding $A^2\Sigma^+$ and the dissociative $^2\Sigma^-$ state. Figure 2 depicts the resonance corresponding to the $F_2$ level ($J_f = N+1$) with $N=2$ and $v=9$ of the $A^2\Sigma^+$ state. ($J_f$ and $v$ are the total angular momentum and vibrational quantum numbers, respectively, and $N$ is the quantum number that describes the Hund's case (b) rotational levels). The total cross section as well as the partial cross sections to each spin orbit component $O(^3P_j, j=0, 1, 2)$ exhibit highly asymmetric features. The initial ground state is the $X^2\Pi^-{}_{2/3}$ state, which is of the lowest energy, with $J_i = 3/2$. The zero of energy is taken as the statistical average of the $O(^3P_j, j=0, 1, 2)$ fine structure splittings. The total cross section does not decay to zero near the resonance, in contrast to the predissociation of $Cs_2$[8] near 580 nm, since there is more than one (at least three repulsive states $^4\Sigma^-$, $^2\Sigma^-$ and $^4\Pi$) continuum state involved in the predissociation precess.[6] More importantly, the partial cross sections show different degrees of asymmetry, represented by different values of the parameter $q$.[6] The asymmetry of the partial cross sections to $O(^3P_0)$ can be understood easily, since the $^2\Sigma^-$ state correlates with this oxygen fine structure component,[14] and since this state is optically coupled with the ground $X^2\Pi$ state. However, it is very intriguing that the partial cross sections to $O(^3P_1)$ and to $O(^3P_2)$ exhibit asymmetric resonances as well, since the $^4\Sigma^-$ and $^4\Pi$ states, whose spin-orbit components dissociate to $O(^3P_j, j=1, 2)$ states,[14] do not carry oscillator strengths from the $X^2\Pi$ state. One possibility is that the $^4\Sigma^-$ and $^4\Pi$ states may borrow intensity from the bright $^2\Sigma^-$ state by continuum-continuum interactions[15,16] among these dissociative states. Further investigations are under way.

**Acknowledgment.** This work has been supported by the Non Directed Research Fund, Korea Research Foundation, 1994.

## References

1. Singer, S. J.; Freed, K. F.; Band, Y. B. *Adv. Chem. Phys.* **1985**, *61*, 1.
2. Williams, C. J.; Freed, K. F. *J. Chem. Phys.* **1986**, *85*, 2699.
3. Band, Y. B.; Freed, K. F.; Kouri, D. J. *Chem. Phys. Lett.* **1981**, *79*, 233.
4. Singer, S. J.; Freed, K. F.; Band, Y. B. *J. Chem. Phys.* **1984**, *81*, 3091.
5. Struve, W. S.; Singer, S. J.; Freed, K. F. *Chem. Phys. Lett.* **1984**, *110*, 588.
6. Fano, U. *Phys. Rev.* **1961**, *124*, 1866.
7. Glass-Maujean, M.; Breton, J.; Guyon, P. M. *Chem. Phys. Lett.* **1979**, *63*, 591.
8. Kim, B.; Yoshihara, K.; Lee, S. *Phys. Rev. Lett.* **1994**, *73*, 424.
9. Brandon, J. T.; Reid, S. A.; Robie, D. C.; Reisler, H. *J. Chem. Phys.* **1992**, *97*, 5246.
10. Lee, S.; Williams, C. J.; Freed, K. F. *Chem. Phys. Lett.* **1986**, *130*, 271.
11. (a) Lee, S. *Chem. Phys. Lett.* (in press). (b) Lee, S. *J. Chem. Phys.* (in press). (c) Lee, S. *Bull. Kor. Chem. Soc.* (in press).
12. Johnson, B. R. *J. Chem. Phys.* **1977**, *67*, 4086.
13. Cooley, J. W. *Math. Comp.* **1961**, *383*, 15.
14. Bazet, J. F.; Harel, C.; McCarroll, R. *Astro. Astrophys.* **1975**, *43*, 223.
15. Lee, S. (submitted for publication).
16. Lee, S.; Park, C. R.; Kim, H. L.; Park, S. C. *Chem. Phys. Lett.* **1995**, *233*, 207.

## Observation of Charge Transfer in $Eu^{3+}$-Aliphatic Carboxylate Mixtures

Jin Sup Hong, Jeong-A Yu†, and Kang-Jin Kim*

*Department of Chemistry, Korea University, Seoul 136-701, Korea*
†*Department of Science Education, Chosun University, Kwangju 501-140, Korea*

*Received February 11, 1995*

Studies on the luminescence intensity of lanthanide ions ($Ln^{3+}$) have been topics of great interest to numerous physical, chemical and biological systems.[1,2] Since the absorption cross sections of $Ln^{3+}$ are small within the uv-visible spectral region,[3] a primary mechanism of luminescence from $Ln^{3+}$ involves their sensitization by organic chelates.[4] In the previous work,[5] we reported the luminescence properties of PSMA-$Ln^{3+}$ (Ln=Tb, Eu, Dy, Yb, Gd) complexes in aqueous solution, where PSMA stands for the sodium salt of styrene and maleic acid copolymer.

By considering spectral overlap integrals,[6] unlikely low efficiencies of energy transfer from the styryl moieties to $Eu^{3+}$ in PSMA-$Eu^{3+}$ was obtained as compared with PSMA-$Tb^{3+}$. Although a charge transfer (CT) band was not clearly observed, we proposed that the insignificant sensitized emission arises because of a low-lying ligand-to-$Eu^{3+}$ CT band. The CT states were suggested to be the most effective acceptor states in many ligand-to-$Eu^{3+}$ electronic energy transfer processes occurring in the near uv spectral range, and their existence accounted for the relatively large quenching efficiencies of $Eu^{3+}$ toward intrinsic ligand luminescence.[7] To obtain the effectively sensitized emission from $Eu^{3+}$, better understanding of the energies of CT band is essential.

In this communication, we report the finding of CT bands in $Eu^{3+}$ and some simple aliphatic carboxylate mixtures. Absorption spectra were recorded on a Hewlett Packard 8542A diode array spectrophotometer, and luminescence measurements were carried out by a Hitachi 650-60 spectrofluorimeter. Chloride salts of lanthanide ions (purity of 99.9% or greater from Aldrich) were used without further purification. All other chemicals of GR grade were used as received.

The absorption and excitation spectra of $Eu^{3+}$, sodium acetate, and $Eu^{3+}$-acetate mixture in aqueous solution are shown in Figure 1. The narrow bands in Figure 1b correspond to metal centered $4f \rightarrow 4f$ transitions,[8] which could be hardly observed in the absorption spectra (Figure 1a). Mixtures of acetate in the form of sodium salt and $Eu^{3+}$ exhibit